Published in final edited form as:
Magn Reson Med. 2009 April ; 61(4): 828–833. doi:10.1002/mrm.21793.

Sensitivity of MR Diffusion Measurements to Variations in Intracellular Structure: Effects of Nuclear Size

Junzhong Xu[1,2], **Mark D. Does**[1,3,4], and **John C. Gore**[1,2,3,4,5,*]

John C. Gore: john.gore@vanderbilt.edu

[1] Institute of Imaging Science, Vanderbilt University, Nashville, TN 37232, USA

[2] Department of Physics and Astronomy, Vanderbilt University, Nashville, TN 37232, USA

[3] Department of Biomedical Engineering, Vanderbilt University, Nashville, TN 37232, USA

[4] Department of Radiology and Radiological Sciences, Vanderbilt University, Nashville, TN 37232, USA

[5] Department of Molecular Physiology and Biophysics, Vanderbilt University, Nashville, TN 37232, USA

Abstract

Magnetic resonance imaging measurements of the apparent rate of water diffusion in tumors are sensitive to variations in tissue cellularity, which have been shown useful for characterizing tumors and their responses to treatments. However, because of technical limitations on most MRI systems, conventional pulse gradient spin echo (PGSE) methods measure relatively long time scales, during which water molecules may encounter diffusion barriers at multiple spatial scales, including those much greater than typical cell dimensions. As such they cannot distinguish changes on sub-cellular scales from gross changes in cell density. Oscillating gradient spin echo (OGSE) methods have the potential to distinguish effects on restriction at much shorter time and length scales. Both PGSE and OGSE methods have been studied numerically by simulating diffusion in a three-dimensional, multi-compartment tissue model. The results show that conventional measurements with the PGSE method cannot selectively probe variations over short length scales and, therefore, are relatively insensitive to intracellular structure, whereas results using OGSE methods at moderate gradient frequencies are affected by variations in cell nuclear sizes and can distinguish tissues that differ only over sub-cellular length scales. This additional sensitivity suggests that OGSE imaging may have significant advantages over conventional PGSE methods for characterizing tumors.

Keywords

MRI; diffusion; cancer; intracellular; nuclear size

Introduction

Diffusion-weighted magnetic resonance imaging (DWI) is sensitive to the rate of diffusion of water molecules in tissues, and has been used to provide information on tissue structure at sub-voxel levels (1–3). DWI can provide diagnostic insights into various pathologies such as stroke (4), and consequently has become an established clinical technique. In both animal

*Correspondence to John C. Gore, Vanderbilt University Institute of Imaging Science, 1161 21st Ave. South, AAA-3017 MCN, Nashville, TN 37232-2310.

and clinical studies, measurements of the apparent diffusion coefficient (ADC) of water have also been shown to provide information on the state of tumors and their response to treatments by revealing tissue characteristics such as tumor cellularity (5–8). Tumor cellularity is usually interpreted to mean cell density, though it may be measured histologically in terms of the integrated area of nuclei of cells divided by the total area of the histologic section. Regions with high cell density tend to have a lower ADC than regions with a low cellularity (7). This correlation makes ADC a potentially powerful biomarker for characterizing tumors and their early response to treatment. However, malignant tumors do not always have higher cellularities than normal tissues or benign tumors. For example, Guo *et al.* (9) found that a malignant scirrhous breast adenocarcinoma had a lower cellularity and elevated ADC compared to normal tissues, whereas a benign papilloma showed a higher cellularity and a lower ADC. Nonetheless, in these examples the inverse relationship of cellularity and ADC was conserved. This correlation in practice is actually a relationship between ADC and cell density. Conventional ADC measurements on MRI systems use the pulsed gradient spin echo (PGSE) method, in which gradients are applied in pairs, separated by a diffusion interval. Because of hardware limitations, and in order to impart sufficient diffusion weighting to be able to see significant signal reductions, the diffusion intervals used in practice are relatively long, typically several 10's of milliseconds (10). From the Einstein relationship, in a time of e.g. 40 ms, free water molecules with an intrinsic diffusion coefficient of 2.5×10^{-5} cm^2sec will move a distance on average ≈ 24 microns, which is larger than the dimension of most cells. The measured values of water ADC in many tissues are ≈ 5 times lower, suggesting that water diffusion in tissues is restricted. Such restrictions are caused, for example, by structures such as cell membranes, which have limited permeability. Conventional measurements of ADC made using long diffusion intervals represent the integrated effects of obstructions to free diffusion at all scales up to the limiting value determined (as above) by the experimentally-selected diffusion interval. As such they may be dominated by obstructions at large scales, such as cell membranes, which reflect overall cell density, and they cannot distinguish these from restrictions that occur at smaller scales, such as those associated with intracellular structures. The observed relation between ADC and cellularity in conventional DWI measurements is likely a reflection of the effects of water molecules encountering different numbers of cell membranes in a specific time, and no separate information can be obtained about structural variations on sub-cellular scales. Although cell density may still be clinically useful as an indicator of tumor aggressiveness or metastatic capacity (11), it is plausible that more specific insights into tumor status may be provided by developing methods that are sensitive to intracellular properties.

Several authors have suggested that assessments of the sizes of tumor cell nuclei may be useful for diagnostic purposes (12,13). Indeed, nuclear anaplasia is a diagnostic feature of many malignancies and often represents the consequence of major changes in biochemical composition. A larger cell nuclear size usually means a more aggressive (high grade) tumor (14). In order to make diffusion measurements sensitive specifically to features such as nuclear size, they must be performed with diffusion times that are much shorter than those in common use. One approach to reduce diffusion times is the oscillating gradient spin echo (OGSE) method (15,16). In OGSE measurements, the conventional bipolar gradient pair is replaced with a matched pair of sinusoidally or cosinusoidally oscillating gradients, which thereby measure the diffusion behavior on the time scale of the period of each oscillation, which may be much shorter than the diffusion interval in typical PGSE methods. The gradients commonly available on MRI systems can readily oscillate at frequencies of the order of a kilohertz, so that diffusion times can be achieved that are at least an order of magnitude shorter than with typical PGSE measurements. These in turn imply that OGSE measurements can be made much less sensitive to large scale restriction effects and thereby be more selectively sensitive to intracellular changes.

In the present work, the feasibility of using OGSE diffusion measurements to obtain information on cell nuclear sizes was evaluated numerically using an improved finite difference method to simulate water diffusion within a 3D multi-compartment tissue model. The results show that conventional PGSE methods with typical choices of parameters can barely distinguish tissues with different nuclear sizes if the cell densities are the same, consistent with the view that conventional ADC measurements are dominated by cell density and are insensitive to intracellular structures. By contrast, the OGSE method can differentiate tissues with the same cell density but which differ over only very short length scales, which means the OGSE method can be much more sensitive to variations in intracellular structure such as nuclear sizes. Moreover, the simulations show that the degree of contrast produced by variations in ADC at high gradient frequencies (short diffusion times) that arise from variations in cell nuclear size are significantly greater than obtainable with PGSE methods. Thus OGSE measurements should prove more sensitive and specific for many purposes in their applications to tumor characterization. The effect of the choice of gradient amplitude in the OGSE method has also been studied, which can be helpful for selecting parameters in experimental applications.

Materials and methods

Oscillating gradient spin echo (OGSE) method

We have simulated an adaptation of the OGSE method that was originally suggested by Gross and Kosfeld (17). Callaghan and Stepisnik analyzed spin diffusive motion in the frequency domain using oscillating gradients (18), and showed that the DWI signal is dependent on the frequency of the applied gradient, namely,

$$S = S_0 \exp\left(-\frac{1}{\pi}\int_o^\infty \mathbf{F}(\omega)\mathbf{D}(\omega)\mathbf{F}(\omega)d\omega\right), \quad [1]$$

where $\mathbf{D}(\omega)$ is the diffusion spectrum and $\mathbf{F}(\omega)$ is the Fourier transform of the time integral of gradient

$$\mathbf{F}(\omega) = \int_{-\infty}^{\infty} dt' \exp(i\omega t') \int_0^{t'} dt'' \gamma g(t''). \quad [2]$$

A higher frequency corresponds to a smaller effective diffusion time, and a gradient waveform with more high frequency and fewer low frequency components will be more specific for probing shorter diffusion times. If $g(t) = G\cos(\omega_0 t)$, $\mathbf{F}(\omega) = \frac{i\pi G}{\omega_0}[\delta(\omega - \omega_0) - \delta(\omega + \omega_0)]$ and the gradient spectrum has no zero-frequency component (19) and probes a well defined diffusion regime. Therefore, a cosine-modulated gradient was used in the present work to obtain a short diffusion time and the corresponding b values can be expressed as

$$b = \frac{\gamma^2 G^2 \sigma}{4\pi^2 f^2}, \quad [3]$$

where γ is the proton gyromagnetic ratio, G the gradient amplitude, f the gradient frequency, and σ is the duration of one gradient series (There are identical gradient series on both sides of the 180 pulse). The b value determines the degree of signal reduction induced by diffusion in the presence of the gradient viz.

$$S = S_0 \exp(-bD) \quad [4]$$

where S, S_o are the measured NMR signals with and without the applied gradients respectively.

In practice, in order to remove the sharp pulse edges at the start and the end of a cosine-modulated gradient, an apodised cosine-modulated gradient waveform is used, which replaces the first and the last one quarter of the cosine- by a half sine-pulse at twice the base frequency (10,16). The corresponding b values can be expressed as

$$b = \frac{\gamma^2 G^2 \sigma}{4\pi^2 f^2}\left(1 - \frac{1}{8N}\right), \quad [5]$$

where N is the number of cycles in each gradient series.

Finite difference simulations

An improved finite difference method (20) was used in our simulation to calculate the evolution of the NMR signals. This method rewrites the Bloch-Torrey equation for transverse magnetization in a matrix form as (for simplicity, only 1D formulae are considered below, but 2D and 3D cases can be easily derived in a similar way.)

$$\mathbf{M}^{n+1} = \mathbf{\Phi}^n \otimes (\mathbf{I} + \mathbf{A})\mathbf{M}^n, \quad [6]$$

where n denotes the temporal index, $\mathbf{M}$ is transverse magnetization, $\mathbf{I}$ is an identity matrix with the same size of $\mathbf{A}$, $\otimes$ denotes the element-by-element vector multiplication and $\mathbf{\Phi}_n$ is a vector describing the phase accumulation and the transverse relaxation in every time step,

$$\mathbf{\Phi}^n = \left[\exp(-i\gamma g^n x_1 \Delta t - \Delta t/T_{2,1}), \exp(-i\gamma g^n x_2 \Delta t - \Delta t/T_{2,2}), \cdots, \exp(-i\gamma g^n x_N \Delta t - \Delta t/T_{2,N})\right] \quad [7]$$

and

$$\mathbf{A} = \begin{pmatrix} -s_{1\to 2} - s_{1\to N} & s_{2\to 1} & 0 & \cdots & s_{N\to 1}\exp(i\alpha\gamma\sum_{k=1}^{n} g^k \Delta t) \\ s_{1\to 2} & -s_{2\to 1} - s_{2\to 3} & s_{3\to 2} & \cdots & 0 \\ 0 & s_{2\to 3} & -s_{3\to 2} - s_{3\to 4} & \cdots & 0 \\ \vdots & \vdots & \vdots & \ddots & 0 \\ s_{1\to N}\exp(-i\alpha\gamma\sum_{k=1}^{n} g^k \Delta t) & 0 & 0 & \cdots & -s_{N\to N-1} - s_{N\to 1} \end{pmatrix}, \quad [8]$$

where $S_{i\rightarrow j}$ is the jump probability from point (*i*) to (*j*) (21). Note that a revised periodic boundary condition is included, which removes the computational edge effect artifact found using the conventional finite difference method. To further enhance the computing efficiency, a tightly coupled parallel computing solution was also implemented. Further details of the computational aspects of our method have been reported previously and can be found in Ref.(20).

A 3D multi-compartment tissue model

A simplified 3D multi-compartment model was used to simulate the behavior of water diffusing in tissues (see Fig. 1). The tissue is considered as a close-packed system of spherical cells. Each cell contains a central spherical nucleus. As a result, there are three distinct compartments containing water in this model, corresponding to intra-nuclear, cytoplasmic and extra-cellular spaces. Each component is ascribed its own intrinsic parameters, including a water self-diffusion coefficient and T_2. The interfaces between the compartments are assumed to be only semi-permeable and are each ascribed a value of permeability to water exchange. Mitochondria and other organelles are not explicitly modeled due to their small sizes. To include the averaged effect on diffusion due to restrictions and/or hindrance of organelles, the intrinsic diffusion coefficient of cytoplasm is given a value smaller than those of nucleus and extra-cellular space. This assumption has been confirmed by experimental observations (22).

The simulation can calculate the behavior of the ADC for a range of values of model parameters, but we here highlight only the results for realistic values relevant for MRI of tumors. We chose to simulate cells with diameters of 10 μm (typical of many human cells). For the results reported here, the cell size and spacing were kept constant but the nuclear size was varied so that the ratio of nuclear volume to cell volume (N/C) also varied.

All other simulation parameters were chosen from published experimental results: the cell membrane permeability was taken to be 0.024 μm/ms (23), the intrinsic diffusion coefficients for nucleus = 1.31 μm^2/ms, for cytoplasm = 0.48 μm^2/ms and for the extra-cellular space = 1.82 μm^2/ms (22). For all simulations, b = 1 ms/μm^2 and TE = 40 ms. T_2 was assumed homogeneous everywhere.

In each simulation, the spatial steps for water molecules undergoing random diffusion were $\Delta x = \Delta y = \Delta z = 0.5$ μm and the temporal increment used was $\Delta t = 0.001$ ms. These parameters may be automatically adjusted in case of very high gradient amplitudes in order to keep all computational errors less than 1% (20). All simulations were performed on the computing cluster of the Vanderbilt University Advanced Computing Center for Research & Education. The programs were written in C with MPI (message passing interface) running on 2.0 GHz Opteron processors and a 32-bit Linux operation system with a Gigabit Ethernet network.

Results and Discussion

ADC differences obtained by PGSE and OGSE

Two types of tissue (denoted_I and _II) were simulated. They have the same structures except that the ratio N/C was different (and equals to 6.2% and 22.0%, respectively). The ADCs and percent difference in ADC (ΔADC) between the two tissues are shown in Fig. 2. On the left (Fig. 2a and Fig. 2c) are the results for the PGSE sequence as a function of diffusion time, and on the right (Fig. 2b and Fig. 2d) are the corresponding OGSE results as a function of gradient oscillation frequency. The shaded regions of Fig. 2c and Fig. 2d represent the typically relevant domains of diffusion time (20 – 80 ms) and oscillation frequencies (< 1 kHz).

Over these relevant domains, ADCs measured by PGSE are relatively constant, whereas, ADCs measured by OGSE change substantially. Similarly, ΔADC from PGSE measurements is small (< 3.6 %) and relatively insensitive to diffusion time, while ΔADC from OGSE measurements changes rapidly with increasing frequency and approaches 15 % at 1 kHz. That is, OGSE measurements in this model system reveal approximately 4 times greater percent difference in ADC between tissues that vary only in sub-cellular characteristics.

Fig. 2 also shows the interesting result that the ADC of tissue_II (with larger N/C) is larger than of tissue_I (smaller N/C) at short diffusion times, whereas it becomes smaller at longer diffusion times. At short diffusion times, the overall ADC approaches a weighted average of the intrinsic diffusion coefficients of each compartment. The intrinsic diffusion coefficient of water in the nucleus was assumed to be larger than the diffusion coefficient in the cytoplasm; hence, a larger N/C results in a larger ADC. At long diffusion times, water diffusion is heavily restricted/hindered by membranes and the ADC will be lower when the average water molecules encounters more membranes. With the smaller nucleus, water in tissue_I is more likely to diffuse past the nucleus without encountering its membrane, thereby making the ADC in tissue_I higher than that in tissue_II.

ADCs change with N/C variation

The variation of tissue ADCs as a function of cell nuclear sizes is shown in Fig. 3. The solid line represents the ADCs obtained using the fast exchange approximation (all membranes are freely permeable), which can be considered as the tissue's mean intrinsic diffusion coefficient without any restriction. The dashed lines represent ADCs obtained by the OGSE method (at 200 Hz and 1 kHz). All ADCs obtained by the OGSE method are smaller than the corresponding intrinsic mean diffusion coefficients. The ADCs obtained by the PGSE method, shown as dotted lines in Fig. 3, show no notable changes over a broad range (from 2.9% to 73.7%) of variations of N/C, which is consistent with observation in Fig. 2 that typical PGSE methods are not sensitive to physical changes in tissue at the sub-cellular level. On the other hand, the OGSE-measured ADC changes smoothly and by ≈ 40 % over the same range of N/C, which means that the observations in Fig. 2 were not specific to a narrow range of N/C values. Also note the similarity between the OGSE curves in Fig. 3 and the solid line, which is simply a weighted average of the intrinsic compartment diffusion coefficients. This similarity points to the OGSE more closely measuring intrinsic diffusion coefficients rather than the effects of restrictions on the scale of 10s of μm apart.

Gradient amplitude limitation on OGSE method

The data in Fig. 2 and Fig. 3 were derived using b = 1 ms/μm^2 at all frequencies, which can produce reasonable reductions in MRI signals to detect diffusion effects and permit accurate calculation of ADC values. However, in OGSE, b is proportional to $1/f^2$, and σ is limited by T_2 relaxation; hence, at high frequency it is difficult to achieve high b values with practical gradients. It is, therefore, of interest to assess limits on the OGSE method from constraints on gradient strength in order to help design practical experiments. Fig. 4 shows the maximum contrast between tissue_I and tissue_II in a diffusion weighted OGSE image (cosine gradients) for three different maximum gradient amplitudes. For comparison, the maximum contrast obtained by the PGSE method is also provided and shown as the solid line, assuming the conditions Δ = 40 ms and b = 1 ms/μm^2. The maximum contrast is defined as the absolute value of signal decay difference, namely,

$$\Delta S = |\exp(-b_{max} \cdot ADC_{\text{tissue\_I}}) - \exp(-b_{max} \cdot ADC_{\text{tissue\_II}})|, \quad [9]$$

where b_{max} is the maximum applicable b value for the measurements, and both b_{max} and ADC are gradient frequency dependent in the OGSE method.

The dashed line in Fig. 4 denotes the conditions for G_{max} = 100 G/cm and TE = 40 ms, as might be possible for imaging a mouse on a small animal MRI system. In the low gradient frequency range (< 300 Hz), sufficiently large b values can be obtained so that ΔS is primarily dependent on ADC differences. The ADC difference increases with gradient frequency (see Fig. 2), so ΔS also increases with gradient frequency. However, in the higher gradient frequency range (> 300 Hz), ΔS decreases with frequency because b_{max} is proportional to $1/f^2$. The peak of ΔS appears at around 300 Hz when the maximum practical contrast is obtained in OGSE measurements with these conditions. Note that the peak contrast occurs well below the frequency where the ADC differences level out (Fig. 2), which means that with larger gradient amplitudes, even greater contrast between tissue I and II would be attainable from OGSE.

Likewise, with smaller gradient amplitudes, the advantages of the OGSE are reduced. The dotted curve demonstrates a lesser but still substantial gain in OGSE contrast as compared to PGSE when G_{max} = 40 G/cm and TE = 40 ms, as might be possible for imaging a rat on a small animal MRI system. However, when G_{max} is reduced to 8 G/cm, even with an increase in TE to 80 ms, the dot-dash curve shows that OGSE contrast is not as great as would be obtained by PGSE. Note that the lowest frequency in Fig. 4 is 50 Hz because of the echo time limitation (40 ms). If lower frequencies (< 50 Hz) can be achieved in measurements, it can be expected that the contrasts by OGSE method approach those by PGSE method. Notice that Fig. 4 shows the contrast, but since noise is not changing with gradient frequency, this is proportional to the CNR, from which the uncertainty in estimated ADC can be calculated.

Conclusions

Measurements of the sizes of cell nuclei have been suggested as useful biomarkers of malignant state and tumor grade. Imaging methods that can distinguish such sub-cellular properties are likely useful in the context of evaluating tumors non-invasively. However, due to hardware limitations, conventional measurements of ADC using the PGSE method are dominated by changes in tumor cell densities and are relatively insensitive to variations in diffusion at sub-cellular length scales. By contrast the OGSE method measures remarkable differences between tissues that differ only in terms of intracellular structure. Hence, ADC measurements with the OGSE method should be useful for probing nuclear size variations. This would enhance the ability of diffusion imaging to be used as a biomarker for assessing the state of tumors. Our simulations show that the OGSE method can provide more contrast and be sensitized to changes that are not detectable by conventional PGSE methods. A preliminary experimental study has been recently reported which investigated C6 gliosarcoma in a rat model with OGSE and PGSE, which confirmed that the OGSE method is more sensitive to structural variations within tumors than the PGSE measurements (24). It should be noted that the actual intracellular structural changes that take place in cancerous cells are much more complex than the tissue model considered here. For example the nucleus changes dynamically and the diffusion and relaxation properties may vary during cell division and apoptosis. However, the simple model analyzed above was chosen to demonstrate the feasibility of using OGSE to probe intra-cellular structural changes, such as nuclear size variations. Moreover, the lack of available experimental data makes it difficult to more precisely model diffusion changes during cell proliferation and apoptosis. Here, all diffusion coefficients are assumed constant in the present work. These techniques can be readily implemented on current small animal

scanners, though their use in humans will be limited using present gradient systems. These simulations provide a useful background for ongoing and future experimental studies.

Acknowledgments

This work was funded by NIH grants CA109106 and NS034834. The simulations used the resources of the Advanced Computing Center for Research and Education (ACCRE) at Vanderbilt University, Nashville, TN.

Grant Support: NIH CA109106 and NS034834

References

1. Cory DG, Garroway AN. Measurement of translational displacement probabilities by NMR: an indicator of compartmentation. Magn Reson Med. 1990; 14(3):435–444. [PubMed: 2355827]
2. Assaf Y, Mayk A, Cohen Y. Displacement imaging of spinal cord using q-space diffusion-weighted MRI. Magn Reson Med. 2000; 44(5):713–722. [PubMed: 11064406]
3. Chin CL, Wehrli FW, Fan Y, Hwang SN, Schwartz ED, Nissanov J, Hackney DB. Assessment of axonal fiber tract architecture in excised rat spinal cord by localized NMR q-space imaging: simulations and experimental studies. Magn Reson Med. 2004; 52(4):733–740. [PubMed: 15389948]
4. Moseley ME, Cohen Y, Mintorovitch J, Chileuitt L, Shimizu H, Kucharczyk J, Wendland MF, Weinstein PR. Early detection of regional cerebral ischemia in cats: comparison of diffusion- and T2-weighted MRI and spectroscopy. Magn Reson Med. 1990; 14(2):330–346. [PubMed: 2345513]
5. Zhao M, Pipe JG, Bonnett J, Evelhoch JL. Early detection of treatment response by diffusion-weighted 1H-NMR spectroscopy in a murine tumour in vivo. Br J Cancer. 1996; 73(1):61–64. [PubMed: 8554985]
6. Chenevert TL, McKeever PE, Ross BD. Monitoring early response of experimental brain tumors to therapy using diffusion magnetic resonance imaging. Clin Cancer Res. 1997; 3(9):1457–1466. [PubMed: 9815831]
7. Sugahara T, Korogi Y, Kochi M, Ikushima I, Shigematu Y, Hirai T, Okuda T, Liang L, Ge Y, Komohara Y, Ushio Y, Takahashi M. Usefulness of diffusion-weighted MRI with echo-planar technique in the evaluation of cellularity in gliomas. J Magn Reson Imaging. 1999; 9(1):53–60. [PubMed: 10030650]
8. Gauvain KM, McKinstry RC, Mukherjee P, Perry A, Neil JJ, Kaufman BA, Hayashi RJ. Evaluating pediatric brain tumor cellularity with diffusion-tensor imaging. AJR Am J Roentgenol. 2001; 177(2):449–454. [PubMed: 11461881]
9. Guo Y, Cai YQ, Cai ZL, Gao YG, An NY, Ma L, Mahankali S, Gao JH. Differentiation of clinically benign and malignant breast lesions using diffusion-weighted imaging. J Magn Reson Imaging. 2002; 16(2):172–178. [PubMed: 12203765]
10. Does MD, Parsons EC, Gore JC. Oscillating gradient measurements of water diffusion in normal and globally ischemic rat brain. Magnetic Resonance in Medicine. 2003; 49(2):206–215. [PubMed: 12541239]
11. Lyng H, Haraldseth O, Rofstad EK. Measurement of cell density and necrotic fraction in human melanoma xenografts by diffusion weighted magnetic resonance imaging. Magn Reson Med. 2000; 43(6):828–836. [PubMed: 10861877]
12. Arai Y, Okubo K, Terada N, Matsuta Y, Egawa S, Kuwao S, Ogura K. Volume-weighted mean nuclear volume predicts tumor biology of clinically organ-confined prostate cancer. Prostate. 2001; 46(2):134–141. [PubMed: 11170141]
13. Hsu CY, Kurman RJ, Vang R, Wang TL, Baak J, Shih Ie M. Nuclear size distinguishes low- from high-grade ovarian serous carcinoma and predicts outcome. Hum Pathol. 2005; 36(10):1049–1054. [PubMed: 16226103]
14. Zink D, Fischer AH, Nickerson JA. Nuclear structure in cancer cells. Nat Rev Cancer. 2004; 4(9): 677–687. [PubMed: 15343274]

15. Schachter M, Does MD, Anderson AW, Gore JC. Measurements of restricted diffusion using an oscillating gradient spin-echo sequence. Journal of Magnetic Resonance. 2000; 147(2):232–237. [PubMed: 11097814]

16. Parsons EC, Does MD, Gore JC. Modified oscillating gradient pulses for direct sampling of the diffusion spectrum suitable for imaging sequences. Magnetic Resonance Imaging. 2003; 21(3–4): 279–285. [PubMed: 12850719]

17. Gross B, Kosfeld R. Anwendung der spin-echo-methode der messung der selbstdiffusion. Messtechnik. 1969; 77:171–177.

18. Callaghan PT, Stepisnik J. Frequency-Domain Analysis of Spin Motion Using Modulated-Gradient Nmr. Journal of Magnetic Resonance Series A. 1995; 117(1):118–122.

19. Parsons EC Jr, Does MD, Gore JC. Temporal diffusion spectroscopy: theory and implementation in restricted systems using oscillating gradients. Magn Reson Med. 2006; 55(1):75–84. [PubMed: 16342147]

20. Xu J, Does MD, Gore JC. Numerical study of water diffusion in biological tissues using an improved finite difference method. Phys Med Biol. 2007; 52(7):N111–126. [PubMed: 17374905]

21. Hwang SN, Chin CL, Wehrli FW, Hackney DB. An image-based finite difference model for simulating restricted diffusion. Magn Reson Med. 2003; 50(2):373–382. [PubMed: 12876714]

22. Grant SC, Buckley DL, Gibbs S, Webb AG, Blackband SJ. MR microscopy of multicomponent diffusion in single neurons. Magn Reson Med. 2001; 46(6):1107–1112. [PubMed: 11746576]

23. Anderson AW, Xie J, Pizzonia J, Bronen RA, Spencer DD, Gore JC. Effects of cell volume fraction changes on apparent diffusion in human cells. Magnetic Resonance Imaging. 2000; 18(6): 689–695. [PubMed: 10930778]

24. Colvin DC, Yankeelov TE, Does MD, Yue Z, Quarles C, Gore JC. New Insights into Tumor Microstructure Using Temporal Diffusion Spectroscopy. Cancer Res. 2008; 68(14)

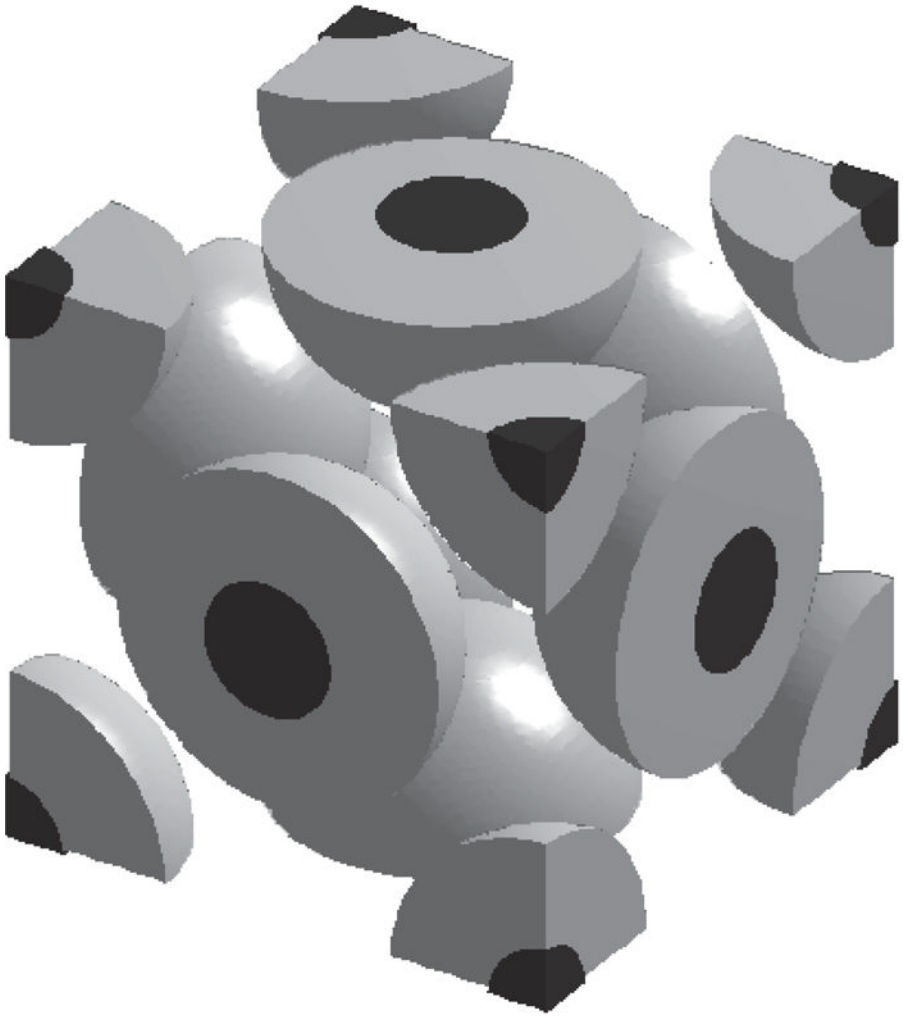

Fig. 1.

Schematic diagram of a simplified 3D tissue model. Black regions represent cell nuclei, gray regions represent cytoplasm and the space outside the spherical cells are extracellular space. Each compartment has its own intrinsic parameters, such as diffusion coefficient. Interfaces between different compartments have permeabilities to mimic cell membranes and nuclear envelopes. Note that the whole tissue is periodic but only a unit cell (shown above) was needed in the simulation, which implemented a revised periodic boundary condition in an improved finite difference method.

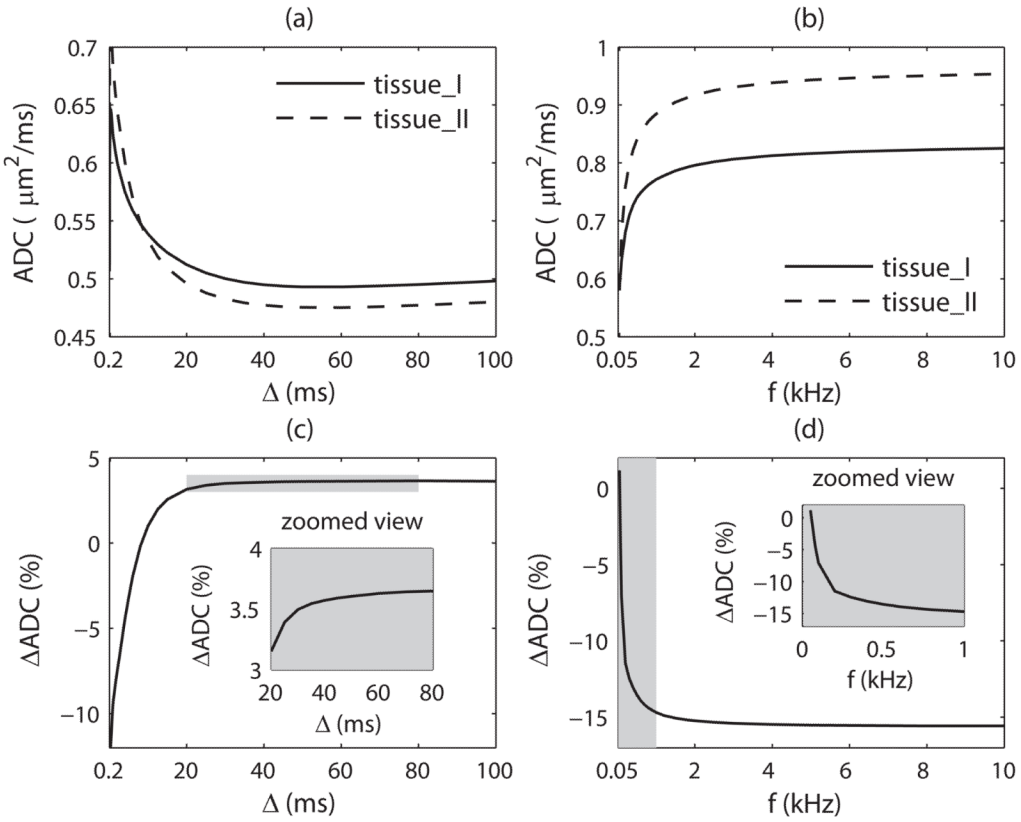

Fig. 2.

Simulated ADCs and ADC differences of two different tissues (N/C 6.2% and 22.0%, respectively). (a) Simulated ADCs with respect to diffusion times by the PGSE method. (b) Simulated ADCs with respect to frequencies of applied oscillating gradients in the OGSE method. (c) ADC differences of two tissues by the PGSE method. The shaded region shows the applicable diffusion time range in typical PGSE measurements. (d) ADC differences of two tissues by the OGSE method. The shaded region shows the applicable oscillating gradient frequency range in typical OGSE measurements.

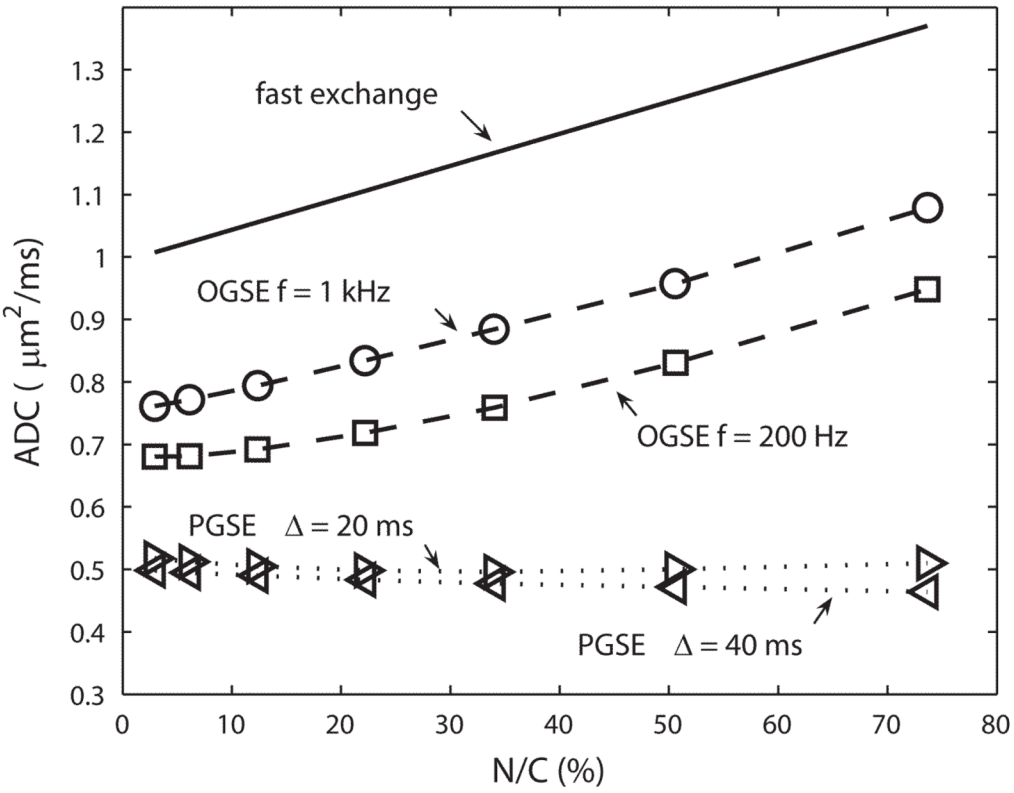

Fig. 3.

Simulated ADCs change with the variation of N/C (the ratio of nuclear volume to cell volume). The solid line represents the ADCs with the fast exchange approximation. The dotted lines and dashed lines represent ADCs obtained by the PGSE method and OGSE methods, respectively.

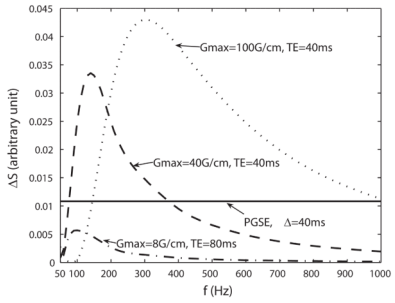

Fig. 4.

Maximum contrast for the OGSE method between tissue_I and tissue_II as a function of gradient frequency in three typical cases. G_{max} is the gradient amplitude. The dashed line denotes the conditions for studies on small animal scanners with G_{max} = 100 G/cm and TE = 40 ms; the dotted line represents diffusion studies with G_{max} = 40 G/cm and TE = 40 ms; the dash-dot line depicts the conditions for *in vivo* diffusion studies on human scanners with G_{max} = 8 G/cm and TE = 80 ms. For comparison, signal contrast obtained by the PGSE method at Δ = 40 ms and b = 1 ms/μm^2 is also showed as the solid line.